Final Report

To

NASA Ames Research Center

NCC2-5208

PRESSURE AND TEMPERATURE SENSITIVE PAINT MEASUREMENTS ON ROTORS

John Sullivan
School of Aeronautics and Astronautics
1282 Grissom Hall
West Lafayette, IN 47907-1282

Temperature and Pressure Sensitive Paints On Rotors

John P. Sullivan
School of Aeronautics and Astronautics
Purdue University
West Lafayette, Indiana 47907-1282

Summary

Luminescent molecular probes imbedded in a polymer binder form a temperature or pressure paint. On excitation by light of the proper wavelength, the luminescence, which is quenched either thermally or by oxygen, is detected by a camera or photodetector. From the detected luminescent intensity, temperature and pressure can be determined. The basic photophysics, calibration, accuracy and time response of a luminescent paints is described followed by applications in wind tunnels and in rotating machinery.

Introduction

The use of luminescent molecular probes for measuring surface temperature and pressure on wind tunnel models and flight vehicles offers the promise of enhanced spatial resolution and lower costs compared to traditional techniques. These new sensors are called temperature-sensitive paint (TSP) and pressure-sensitive paint (PSP). Traditionally, arrays of thermocouples and pressure taps have been used to obtain surface temperature and pressure distributions. These techniques can be very labor-intensive and model/flight vehicle preparation costs are high when detailed maps of temperature and pressure are desired. Further, the spatial resolution is limited by the number of instrumentation locations chosen. By comparison, the TSP and PSP techniques provide a way to obtain simple, inexpensive, full-field measurements of temperature and pressure with much higher spatial resolution. Both TSP and PSP incorporate luminescent molecules in a paint which can be applied to any aerodynamic model surface. Figure 1 shows a schematic of a paint layer incorporating a luminescent molecule.

The paint layer is composed of luminescent molecules and a polymer binder material. The resulting 'paint' can be applied to a surface using a brush or sprayer. As the paint dries, the solvent evaporates and leaves behind a polymer matrix with luminescent molecules embedded in it. Light of the proper wavelength to excite the luminescent molecules in the paint is directed at the model and luminescent light of a longer wavelength is emitted by the molecules. Figure 2 shows the spectra for a typical luminescent ruthenium molecule. Using the proper filters, the excitation light and luminescent emission light can be separated and the intensity of the luminescent light can be determined using a photodetector. Through the photo-physical processes known as thermal- and oxygen-quenching, the luminescent intensity of the paint emission is related to temperature or pressure. Hence, from the detected luminescent intensity, temperature and pressure can be determined.

The polymer binder is an important ingredient of a luminescent paint used to adhere the paint to the surface of interest. In some cases, the polymer matrix is a passive anchor. In other cases, however, the polymer may affect significantly the photophysical behavior of the paint through a complicated interaction between the luminescent molecules and the macro-molecules of the polymer. A good polymer binder should be robust enough to sustain skin friction and other forces on the surface of an aerodynamic model. Also, it must be easy to apply to the surface in a smooth, thin film and easy to repair. For TSPs, many commercially available resins and epoxies can be chosen as polymer binders if they are not oxygen permeable and do not degrade the activity of the luminophore molecules. In contrast, a good polymer binder for a PSP must have high oxygen permeability besides being robust and easy to apply. Two recent papers (Liu et al. 1997 and Gouterman 1997) provide excellent reviews of the foundations and history of TSP and PSP and contain extensive reference lists.

Measurement Systems

The measurement systems are the same for both TSPs and PSPs. The essential elements of the systems include illumination sources, optical filters, photodetectors and data acquisition/processing units. This section provides a brief description of two measurement systems: the CCD camera system and the laser scanning system. Intensity based measurements are considered first and then lifetime and multi-luminophore systems.

CCD Camera System

The CCD camera system for luminescent paints is the most commonly used in aerodynamic testing. A schematic of this system is shown in Figure 3. The luminescent paint (TSP or PSP) is coated on the surface of the model. The paint is excited to luminesce by the illumination source, such as a lamp or a laser. The luminescent intensity image is filtered optically to eliminate the illuminating light and then captured by a CCD camera and transferred to a computer

with a frame grabber board for image processing. Both wind-on image (at temperature and pressure to be determined) and wind-off image (at a known constant temperature and pressure) are obtained. The ratio between the wind-on and wind-off images is taken after the dark current level image is subtracted from both images, yielding a relative luminescent intensity image. Using the calibration relations, the surface temperature and pressure distributions can be computed from the relative luminescent intensity image.

Selection of the appropriate illumination sources depends on the absorption spectrum of the paint and the optical access of the facility. The source must provide a large number of photons in the wavelength band of absorption. A variety of illumination sources are available. Lasers with fiber-optic delivery systems have been used in wind tunnel tests (Morris et al. 1993b, Crites 1993, Bukov et al.. 1992, Engler et al. 1995). Other light sources reported in literature include a xenon arc light with a blue filter (McLachlan et al. 1993a), incandescent tungsten/halogen lamps (Dowgwillo et al. 1994) and fluorescent UV lamps (Liu et al. 1995a, 1995b). Morris et al. (1993a) and Crites (1993) discussed the characteristics of some illumination sources. For imaging the surface, scientific grade cooled CCD digital cameras can provide high intensity resolution (12 and 16 bits) and high spatial resolution (up to 2048 × 2048 pixels). Since the scientific grade CCD camera exhibits good linearity and high signal-to-noise ratio (SNR), it is particularly suitable to quantitative luminescent intensity measurements.

A necessary step in data processing is taking the ratio between the wind-on luminescence image and the wind-off reference image at a known reference temperature and pressure. The image ratio process can eliminate the effects of spatial non-uniformity in illumination light, coating thickness, and luminophore concentration. However, since aerodynamic forces may cause model motion and deformation in high-speed wind tunnel tests, the wind-on image may not align with the wind-off image. The ratio between the non-aligned images leads to considerable errors in calculating temperature and pressure using the calibration relations. Also, some distinct flow characteristics, such as shocks, transition and separation locations, could be smeared. In order to correct this non-alignment, an image registration method was suggested by Bell and McLachlan (1996) and Donovan et al. (1993).

Laser Scanning System

A laser scanning system for TSPs and PSPs is shown in Figure 4. A low power laser is focused to a small point and scanned over the surface of the model using computer controlled mirrors The laser illumination excites the paint on the model and luminescence is detected by a low noise photodetector (e.g. a PMT). The photodetector signal is digitized with a high resolution A/D converter and processed to obtain temperature and pressure. The mirror is synchronized to the data acquisition so that the position of the laser spot on the model is accurately known.

Compared with the CCD camera system, it takes longer to obtain full-surface temperature and pressure distributions using the laser scanning system. However, this system has some advantages. (Hamner et al. 1994)

(i) Luminescence is detected by a low noise photodetector. Before the analog output from the PMT is digitized, filtering and other SNR enhancement techniques are available to improve the measurement resolution. The signal is then digitized with a high resolution (12 to 24 bit) A/D converter. Additional noise reduction can be accomplished by using a lock-in amplifier if the laser intensity is modulated.

(ii) The laser scanning system can be used for measurement in a facility where optical access is very limited and the CCD camera system is difficult to use.

(iii) The system provides uniform illumination over the surface by scanning a single light spot.

(iv) The system can be easily adapted for measurement of luminescent lifetime or phase shift if a pulsed laser or modulated laser is used.

Lifetime-based detection systems

A promising method for making temperature and pressure measurements is to determine the luminescent lifetime of the paint rather than the luminescent intensity. Compared with the intensity-based method, the greatest advantage of this method is that the lifetime-temperature or -pressure relation is not dependent on illumination intensity. Therefore, the calibration relation is intrinsic for a particular paint and the image ratio process is not required. Also, the lifetime measurement is insensitive to luminophore concentration, paint thickness, photodegradation, tubid paint surface and dirty optical surfaces. The temperature and pressure can be directly obtained from the measured lifetime. The lifetime measurement technique in photochemistry is well-developed (Szmacinski and Lakowicz 1995, Papkovsky 1995). The basic configuration of this system is similar to either the CCD camera or the laser scanning system, except a pulsed excitation light is used. After each pulse, the luminescence decay is detected and acquired by a computer. Then, temperature or pressure is obtained by using the calibration relation. Using a lifetime detection system, Davies et al. (1995) measured the pressure distributions on a cylinder in subsonic flow and on a wedge at Mach 2. Comparison with data obtained by conventional pressure taps was favorable.

A frequency-domain method detects the phase angle between the luminescence emission and harmonically modulated excitation light. If the modulation frequency is fixed, the phase angle is a function of the lifetime and hence is dependent on temperature and pressure. The phase angle can be measured using a lock-in amplifier. Campbell et al. (1994) gave a calibration between phase angle and temperature for Ru(bpy)-Shellac paint at 100 kHz modulation frequency. A simple phase detection system

using blue LED excitation was used to measure surface temperature on an electrically heated steel foil on which a round air jet impinged (Campbell et al. 1994). Torgerson et al. (1996) measured the pressure distribution in a low-speed impinging jet using a laser scanning system with an optical modulator.

Multi-Luminophore System

Use of the normal CCD camera or laser scanning system requires a ratio between the wind-on and wind-off luminescent images. This image ratio method inevitably causes inaccuracy in determining temperature and pressure because the image registration is never perfect. A two-color luminophore paint would eliminate the need for a wind-off reference image. Two-color luminescent TSP is made by combining a temperature-sensitive luminophore with a temperature-insensitive reference luminophore. Similarly, two-color luminescent PSP consists of a pressure-sensitive luminophore with a pressure-insensitive reference luminophore. The probe luminophore and reference luminophore can be excited by the same illumination. However, there is ideally no overlap between the emission spectra of the probe luminophore and reference luminophore such that two color luminescent images can be completely separated by optical filters. The ratio between these two color images can eliminate effects of spatial non-uniformity in illumination, paint thickness and luminophore concentration. Besides the aforementioned combinations, a temperature sensitive luminophore which is not quenched by oxygen can be combined with an oxygen sensitive luminophore. This dual luminophore temperature/pressure paint can be used for temperature correction in PSP measurement. Furthermore, a multi-color PSP can be developed to correct simultaneously the effects of both temperature variation and non-uniformities in lighting, paint thickness and concentration.

Some preliminary experiments indeed indicate that a two-color PSP can correct variations in illumination (Oglesby et al. 1995, Harris and Gouterman 1995). Three pressure sensitive paints with internal temperature sensitive luminophore have also been tested by Oglesby et al. (1996). Their results show that the dual luminophore paint enables point-by-point correction of temperature effects of PSP measurement. Only recently, a two-color PSP was used to measure pressure distribution in a low speed impinging jet (Torgerson et al. 1996).

Temperature Sensitive Paints

This section will describe the photophysics, calibration, accuracy, time response of temperature sensitive paint.

Photophysics

For a TSP, it is assumed that the paint layer is not oxygen-permeable so that $[O_2] = 0$. Hence, the quantum yield is simply given by

$$\Phi = \frac{I}{I_a} = \frac{k_L}{k_L + k_D} = k_L \tau_0 \qquad (1)$$

The deactivation term k_D may be decomposed into a temperature-independent part k_0 and a temperature-dependent part k_1 that is related to thermally activated intersystem crossing (i.e. $k_D \doteq k_0 + k_1$). The rate k_1 can be assumed to have an Arrhenius form (Bennett and McCartin 1966, Schanze et al. (1997)

$$k_1 = C \exp(-E/RT) \qquad (2)$$

where C is a constant, E is the Arrhenius activation energy, R is the universal gas constant and T is the thermodynamic temperature (in Kelvin).

The relation (1) can be approximately written in the simple Arrhenius form

$$\ln \frac{I(T)}{I(T_{ref})} = \frac{E}{R}\left(\frac{1}{T} - \frac{1}{T_{ref}}\right) \qquad (3)$$

Theoretically speaking, the Arrhenius plot of $\ln[I(T)/I(T_{ref})]$ versus 1/T gives a straight line of slope E/R. Tests indicate that the simple Arrhenius relation does fit experimental data over a certain temperature range. However, for some paints, the data may not fully obey the simple Arrhenius relation over a wider range of temperature. As an alternative, the relation between the luminescence intensity and temperature can be expressed in a functional form

$$\frac{I(T)}{I(T_{ref})} = F(T/T_{ref}) \qquad (4)$$

The empirical expression $F(T/T_{ref})$ could be a polynomial, exponential or other functions to fit the experimental data over a certain temperature range. Both (3) and (4) are operational forms of the calibration relation for a TSP used for data reduction in practical applications.

TSP Calibration

In order to quantitatively measure temperature with the TSP coatings, a calibration relating luminescent intensity or lifetime to temperature is needed. A calibration rig consists of a temperature controlled sample and appropriate illumination source and luminescent detector.

Typical temperature dependencies of luminescent intensity are shown in Figure 5 for some TSPs. Several TSPs have high temperature sensitivity in cryogenic temperature range. Others can be used in a temperature range from -20 to 105 ^{0}C. Figure 6 gives a lifetime calibration of two TSPs.

Accuracy

The accuracy of the temperature measurement has been shown to depend primarily on calibration accuracy, but is in the range of 1 degree. (see Liu et al. 1995b for a detailed analysis)

Time Response

There are two characteristic time scales that are related to the time response of the paint. One is the luminescent lifetime which represents an intrinsic physical limit for the achievable temporal resolution of the paint. Luminescent paint usually has a lifetime ranging from 10^{-10} seconds to milliseconds. Another is the time scale of the thermal diffusion in the TSP layer. In a forced convection-

dominated case, the thermal diffusion time can be expressed by $\tau = \rho c \ell / h$, where. ρ is the density, c is the specific heat, ℓ is the paint thickness and h is the convection heat transfer coefficient. In general, the diffusion time is much larger than the lifetimes of most luminescent paints. Therefore, the time response of the luminescent paint is mainly limited by the diffusion processes for both TSP and PSP measurements.

Figure 7 shows a the temperature response of the TSP paint subjected to the pulsed laser heating.(Liu et al.,1995c). The surface temperature increases rapidly after the pulsed laser beam is turned on and then gradually decays due to natural convection. By fitting the experimental data with the asymptotic solutions, it is found that τ_1 = 0.25 ms(heating) and τ_2 = 25 ms (cooling).

TSP Applications

Transition Detection

TSP has also been utilized as an approach to flow transition detection (Campbell 1994, McLachlan et al. 1993b). Since convective heat transfer is much higher in turbulent flow than in laminar flow, TSP can visualize the surface temperature difference between turbulent and laminar regions. In low speed wind tunnel tests, the model is typically heated or cooled to enhance temperature variation across the transition line. Using EuTTA-dope paint, Campbell et al. (1992, 1993) visualized transition patterns on a symmetric NACA 65_4-021 airfoil in a low-speed wind tunnel. (Figure 8). Recently, a cryogenic TSP systems have been developed at Purdue, the University of Florida NASA Langley and National Aerospace Laboratory (NAL), Japan. Several TSP formulations have been successfully used to detect transition on airfoils in a 0.1m transonic cryogenic wind tunnel at the NAL in Japan (Figure 9 from Asai et al. 1997a) and a 0.3m cryogenic wind tunnel at NASA-Langley (Figure 10 from Popernack et al.).

Quantitative Heat Transfer

Global surface heat transfer mapping on a waverider model in Mach 10 flow has been obtained using EuTTA-dope paint (Liu et al. 1995b).

A thin Mylar insulating layer covered the windward side of the model, and EuTTA-dope paint was applied on the insulating layer. The temporal evolution of surface temperature distributions was obtained and then heat flux was calculated using a simple heat transfer model. Figure 11 shows a representative map of heat flux on the windward side of the waverider. The bright and dark regions correspond to high and low heat transfer, respectively. The low heat transfer region near the leading edge corresponds to laminar flow. Transition from laminar to turbulent flow can be easily identified by an abrupt change from low to high heat transfer. Figure 12 shows a typical heat transfer history. The TSP measurement is in good agreement with data obtained by thermocouples.

Pressure Sensitive Paints

This section will describe the photophysics, calibration, accuracy, time response of pressure sensitive paint.

Photophysics

PSP operation is based on the principle that certain fluorescent molecules are quenched by the presence of oxygen. In the molecules of interest, oxygen interacts with the excited molecules and the excess energy is transferred to the oxygen in a collisional process, with no photons being emitted. This process, known as oxygen quenching, is the basis for the pressure sensitive paint method.

Calibration curves for common paint formulations (platinum porphrin, ruthenium complex and perlene/pyrene) are shown in Fig. 13.

The luminescent intensity (I) is proportional to the absorption intensity (I_a) and the quantum efficiency (η)

$$I = I_a \eta . \tag{5}$$

Here, the quantum efficiency is defined as

$$\eta = \frac{k_r}{k_r + k_{nr} + k_q [O_2]}, \tag{6}$$

where k_r is the radiative rate constant, k_{nr} is the non-radiative deactivation rate constant, k_q is the radiative rate constant, and $[O_2]$ is the oxygen concentration. According to Henry's law, the concentration of oxygen is proportional to the oxygen partial pressure (P_{O_2}) and air pressure (P)

$$[O_2] = S P_{O_2} = S a P , \tag{7}$$

where S is the solubility of oxygen and a is the volume fraction of oxygen in air. Combination of Eqs. (5), (6), and (7) yield the well-known Stern-Volmer relation

$$\frac{I_0}{I} = 1 + K P , \tag{8}$$

where I_0 is the luminescent intensity in the absence of oxygen and K is the Stern-Volmer constant defined as

$$K = \frac{k_q S a}{k_r + k_{nr}} .$$

The Stern-Volmer relation connects the luminescent intensity I with air pressure P.

In aerodynamic tests, however, the luminescent intensity I_0 in the absence of oxygen is not known. Therefore, another form of the Stern-Volmer relation is often used, that is,

$$\frac{I_{ref}}{I} = A + B \frac{P}{P_{ref}} \tag{9}$$

where I_{ref} and P_{ref} are the reference intensity and pressure, respectively. The coefficients A and B, which are also called the Stern-Volmer constants, are related to K

$$A = \frac{1}{1 + K P_{ref}} \text{ and } B = \frac{K P_{ref}}{1 + K P_{ref}} .$$

Obviously, a constraint is $A(T_{ref}) + B(T_{ref}) = 1$, where T_{ref} is a reference temperature. The Stern-Volmer relation (9) and its extended forms have been widely used as

operational calibration relations for PSP measurements in aerodynamic tests.

The Stern-Volmer coefficients A and B are temperature-dependent. Temperature affects two physical processes: non-radiative deactivation and oxygen diffusion in a polymer. An Arrhenius model for the non-radiative rate constant k_{nr} is given, that is, $k_{nr} = k_{nr0} + k_{nr1} exp(-E_{nr}/RT)$, where k_{nr0} and k_{nr1} are the non-radiative deactivation rate constants, E_{nr} is the Arrhenius activation energy for the non-radiative process, R is the universal gas constant, and T is the thermodynamic temperature in Kelvin. On the other hand, temperature can also affect the oxygen diffusion in a polymer. For a diffusion-limited quenching reaction, the quenching rate constant k_q is described by the Smoluchowski equation $k_q = 4\pi N p_0 D_q$, where D_q is the diffusion coefficient of the quencher $[O_2]$ in the polymer, N is the number of molecules per millimole, and p_0 is a factor that depends on the quenching mechanism. Furthermore, the diffusion coefficient can be described by an Arrhenius model $D_q = exp(-E_q/RT)$, where E_q is the activation energy for the diffusion of the quencher $[O_2]$.

Based on the above models for k_{nr} and k_q, the Stern-Volmer coefficients $A(T)$ and $B(T)$ can be expressed as

$$A(T) = A(T_{ref})\frac{k_r + k_{nr}(T)}{k_r + k_{nr}(T_{ref})} = A(T_{ref})\frac{1+\xi e^{-E_{nr}/RT}}{1+\xi e^{-E_{nr}/RT_{ref}}}$$

$$B(T) = B(T_{ref})\frac{k_q(T)}{k_q(T_{ref})} = B(T_{ref})e^{-(E_q/RT_{ref})(T_{ref}/T-1)},$$

where $\xi = k_{nr1}/(k_r + k_{nr0})$. For small temperature differences and $\xi >> 1$, the Stern-Volmer coefficients $A(T)$ and $B(T)$ are approximately expressed as linear functions of temperature

$$A(T) = A(T_{ref})\left[1 + \frac{E_{nr}}{RT_{ref}}\left(\frac{T-T_{ref}}{T_{ref}}\right)\right]$$

$$B(T) = B(T_{ref})\left[1 + \frac{E_q}{RT_{ref}}\left(\frac{T-T_{ref}}{T_{ref}}\right)\right]. \qquad (10)$$

The formula (10) has important physical implications. The temperature dependence of $A(T)$ is due to the thermal quenching as in TSP, while the temperature dependence of $B(T)$ is related to the temperature dependence of the oxygen diffusivity in a polymer. In general, the coefficient $B(T)$ has a stronger temperature dependence than $A(T)$. This means that the temperature dependence of PSP is dominated by the temperature effect on the oxygen diffusion process in the polymer. This finding has important implications for the design of low-temperature-sensitive PSP formulations. The low-temperature-sensitive PSP should have a polymer binder with low activation energy E_q for the oxygen diffusion.

For a typical PSP (Bath Ruth + silica gel in GE RTV 118), the calibration results are shown in Fig. 14. The coefficients in Eq. (10) obtained by fitting the experimental data are $A(T_{ref}) = 0.13$, $B(T_{ref}) = 0.87$, $E_{nr}/RT_{ref} = 2.82$, and $E_q/RT_{ref} = 4.32$ over a temperature range from $293K$ to $333K$, where the reference temperature is $T_{ref} = 298K$. Furthermore, the activation energy E_q for the oxygen diffusion and the activation energy E_{nr} for the non-radiative process can be calculated. The estimated values are $E_q = 2.56$ *kcal/mole* and $E_{nr} = 1.67$ *kcal/mole*.

A similar calibration is given in Figure 15 for PtTFPP in polystrene.

Accuracy

To estimate the uncertainty of the PSP measurement with a scientific-grade CCD camera system, Morris et al. (1993a) conducted a series of calibration experiments focused on a proprietary PSP paint sample in a pressure vessel which controlled both the temperature and pressure. After averaging a 32 sequential images to improve the SNR, they found that the minimum pressure resolution near atmospheric pressure (13 to 16 psia) is about ± 0.05 psid for their system. Note that the above uncertainty estimates do not contain the contributions from some major error sources such as the temperature effects and model displacement. The uncertainty of PSP measurements depends strongly on a systematic error source associated with the temperature dependence of the paint. An analysis by Sajben (1993) indicates that the temperature uncertainty dominates the PSP measurement errors. Another major error source is model motion between the wind on and wind off images. To date, it has been necessary to perform an in-situ calibration of the PSP using standard pressure taps on the model in order to obtain reasonable accuracy.

A detailed model and error analysis of a PSP system was recently presented by Liu et al (1999). The model used is shown in Fig.16.

The detector output calculated from this model is

$$V = \Pi_c \Pi_f \beta_{\lambda_l} h q_0 \eta(P,T), \qquad (11)$$

The parameters Π_c and Π_f are related to the imaging system performance and filter parameters, respectively. In PSP applications, the intensity ratio method is currently used as a typical procedure to eliminate effect of spatial variation in illumination intensity. When a ratio between the wind-on and reference wind-off images is taken, air pressure P can be expressed in terms of the system's outputs and other variables

$$P = U_1 \frac{V_{ref}(t,x)}{V(t',x')}\frac{P_{ref}}{B(T)} - \frac{A(T)P_{ref}}{B(T)}, \qquad (12)$$

where

$$U_1 = \frac{\Pi_c}{\Pi_{c\,ref}}\frac{\Pi_f}{\Pi_{f\,ref}}\frac{h(x')}{h_{ref}(x)}\frac{c(x')}{c_{ref}(x)}\frac{q_0(t',X')}{q_{0\,ref}(t,X)},$$

where $x = (x,y)^T$ and $x' = (x',y')^T$ are the coordinates in the wind-off and wind-on images, respectively,

$X=(X,Y,Z)^T$ and $X'=(X',Y',Z')^T$ are the object space coordinates in the wind-off and wind-on cases, respectively, and t and t' are the instants at which the wind-off and wind-on images are taken, respectively. The paint thickness is h(x), paint concentration c(x) and the incident illumination is q(x).

When the uncertainty in pressure is solely dominated by the photon shot noise, the error propagation equation contains only two terms related to V and V_{ref}, and the variance of P is

$$\frac{var(P)}{P^2}=\frac{G\hbar\nu B}{V_{ref}}\left[1+\frac{A(T)}{B(T)}\frac{P_{ref}}{P}\right]^2\left[1+A(T)+B(T)\frac{P}{P_{ref}}\right]$$

where G and B are the gain and bandwidth of the photodetector system.

Assuming that the integration time for a detector such as a CCD camera is $t_{INT}=1/B$. The total number of the photoelectrons collected over the integration time is

$$n_{pe}=\frac{V}{G\hbar\nu B} \tag{13}$$

When the detector achieves the maximum capability such as the full well capacity of a CCD, one obtains the minimum pressure difference that the detector can measure from a single realization of data (or image)

$$\frac{(\Delta P)_{min}}{P}=\frac{1}{\sqrt{(n_{pe\,ref})_{max}}}\left[1+\frac{A(T)}{B(T)}\frac{P_{ref}}{P}\right]\times\left[1+A(T)+B(T)\frac{P}{P_{ref}}\right]^{1/2} \tag{14}$$

where $(n_{pe\,ref})_{max}$ the maximum number of photoelectrons collected by a detector in the reference condition (e.g. the full well capacity of a CCD).

When the full well capacity of a CCD is 500,000 electrons and Bath Ruth + silica-gel in GE RTV 118 is used as a PSP, the minimum pressure uncertainty $(\Delta P)_{min}/P$ is shown in Fig. 17 as a function of P/P_{ref} for different temperatures. It is indicated that an increasing temperature degrades the limiting pressure resolution. Figure 18 shows $\sqrt{(n_{pe\,ref})_{max}}(\Delta P)_{min}/P$ as a function of P/P_{ref} for different values of the Stern-Volmer coefficient $B(T)$. Clearly, a larger $B(T)$ leads to a smaller limiting pressure uncertainty $(\Delta P)_{min}/P$.

This PSP system model provides a framework for estimating various elemental errors and calculating the total uncertainty in PSP measurement. The analysis and modeling yield a general functional relation between the imaging system's output and the performance parameters of the imaging system and the physical properties of PSP (Eq. 12). This relation allows identifying various elemental error sources in PSP measurement and evaluating their sensitivity coefficients in error propagation. The accuracy of PSP measurement is limited by the photon shot noise of a photodetector. When a detector is the photon shot noise limited, a useful formula (Eq.14) is given for the minimum pressure difference that a PSP measurement system can measure. The elemental errors induced by model deformation are estimated, including the uncertainty caused by a change in illumination intensity on the model surface after the model moves with respect to light sources. Other major elemental error sources that have been estimated include temperature effects, calibration errors, temporal variations in luminescence and illumination, spectral variability, and pressure mapping. The total uncertainty contributed by these elemental errors is calculated using the error propagation equation.

Time Response

Based on the transient solution of the diffusion equation, the oxygen diffusion time for a thin PSP coating is on the order of $\tau=\ell^2/D_m$, where ℓ is the coating thickness and D_m is the mass diffusivity of oxygen in the paint layer.

Baron et al. (1993) studied the time response to oxygen concentration changes of several PSPs using a pressure jump apparatus. The PSPs that they investigated are PtOEP in GP-197 and MAX-100 polymer binders and H_2TFPP in Silica-W, Silica-B and TLC binders. They found that the response times for GP-197 and MAX-100 binder are 2.45 s and 0.4 s, respectively. The Silica-W and Silica-B show response times of 11 ms and 1.5 ms, respectively. The response time of the TLC is about 25 μs. Recently, using a similar set-up, Carroll et al. (1996) measured the step response of three PSPs: a proprietary PSP from McDonnell Douglas, PtOEP on a white primer layer, and PtOEP in GP-197. For the McDonnell Douglas paint with thickness ranging from 13 to 35 μm, the response time varies from 0.042 s to 0.42 s. The response time of PtOEP on a white primer layer is 45 ms. For PtOEP in GP-197, the response times are 1.4 s, 1.6 s and 2.6 s for the paint thickness of 22 μm, 26 μm and 32 μm, respectively. Bukov et al. (1992) reported that a proprietary fast-responding PSP coating developed by TsAGI has a time constant of 5 ms. Clearly, the diverse time constants of various PSPs result from the effects of the different polymer diffusivity, coating thickness and structure of the paint.

Figure 19a shows the response of bathophen ruthenium in RTV (about 0.05mm in thickness) to step change of pressure generated by a shock tube. The pressure change is shown on a normalized basis from the minimum to the maximum pressures. The response time of the PSP was 172ms determined from the first order system response. Figure 19b shows the response of Pt(II) meso-tetra(pentafluorophenyl)porphine (PtTFPP) in porous polymer/ceramic composites obtained from Scroggin *et al.*. The response time is 349μs for this PSP. A PSP with anodized aluminum as a binder (AA-PSP) has been developed through joint experiments between Purdue University and National Aerospace Laboratory (Japan). Anodized aluminum has 20 to 100nm micropores

distributed on the anodized aluminum surface, which increase the mass diffusivity of oxygen . Mosharov *et al.* reported that the response time of AA-PSP is in a range of 18 to 90μs depending on the luminophore used and on some features of the anodization process. The pressure response to a step change is shown in Fig. 19c fro the AA-PSP and a comparison is made with PSP with TLC plate (TLC-PSP), which used bathophen ruthenium as a luminophore. The observed response time of AA-PSP was 80μs and that of TLC-PSP was 70μs.

PSP Applications

Most of PSP measurements on aerodynamic models have been conducted in transonic and supersonic wind tunnels. Recently, the PSP technique has been used for pressure measurements in low-speed flows and rotating machinery.

Tests in Wind Tunnels

PSPs have been applied to pressure measurements in wind tunnel tests over a wide range of Mach numbers in order to examine the feasibility of this method. Kavandi et al. (1990) and McLachlan et al. (1993a) tested a two-dimensional airfoil (NACA-0012) over a Mach number range of 0.3 to 0.66. McLachlan et al. (1995a, 1995b) also tested a large generic transport wing/body configuration in transonic Mach number from 0.7 to 0.9. The PSP data not only provide good quantitative chordwise pressure results, but also show complicated two-dimensional pressure maps that would be difficult to deduce from the usual discrete tap data. Some experiments conducted in the McDonnell Douglas Research Laboratories (Morris et al. 1993b) include pressure measurements on a generic wing/body model (Mach number = 2 and angle of attack = 8 degree), a model of a high performance fighter (Mach number = 1.2), and a two-dimensional converging/diverging nozzle. Sellers and Brill (1994) conducted a demonstration test of a PSP in the Arnold Engineering Development Center transonic wind tunnel for an aircraft model. Using fast-responding PSP coatings developed at TsAGI, Troyanovsky et al. (1993) carried out a semi-quantitative pressure visualization for a shock/body interaction in a Mach 8 shock tube with 0.1 s duration, and Borovoy et al. (1995) determined the pressure distributions on a cylinder at Mach 6 in a shock wind tunnel with about 40 ms duration. In general, the PSP technique works well in high Mach number subsonic flows and supersonic flows since static pressure change is typically large. Morris (1995) and Shimbo et al. (1997) measured the pressure on delta wings at low Mach numbers ranging from 0.05 to 0.2. These results indicate the low pressure regions induced by leading edge vortices.

Figure 20 shows a typical surface pressure map in the interaction of a cylinder mounted normal to a flat floor with a supersonic turbulent boundary layer at a freestream Mach number of 2.5. In this test carried out in the Purdue University supersonic wind tunnel, the incoming boundary layer thickness is 4 mm, the cylinder height is 15 mm, and the cylinder diameter is 4.8 mm. The PSP, Ru(ph_2-phen) in GE RTV 118, was applied to the floor surface for pressure measurement. The pressure map clearly indicates a pressure rise induced by a bow shock ahead the cylinder and a low pressure region in the turbulent wake behind the cylinder.

Transonic Airfoil - Lifetime Method

The laser scanning method for pressure and temperature sensitive paints was demonstrated in the Boeing Company model transonic wind tunnel. (Torgerson 1997) The arifoil was 10% thick with a sharp leading edge and a small amount of camber. It had 19 pressure taps along the upper surface to compare with the pressures found from the paints. The laser used was a small air-cooled argon-ion laser. The beam was modulated using an electro-optic modulator, enabling the signal to be processed by a two phase lock-in amplifier. Both intensity and phase were recorded during the scan over the airfoil, so that a comparison between intensity and lifetime methods could be made. Results in Figure 21 show both methods compare favorably with the pressure tap data. The phase measurements have the advantage that wind off data is not required.

Rotating Machinery

PSP is a promising non-contact technique for measuring surface pressure distributions on high-speed rotating blades in rotating machinery where conventional instrumentation is particularly difficult. PSP measurements on rotating machinery were conducted by Burns and Sullivan (1995) with a laser scanning system. They obtained the pressure distributions on a small wooden propeller at a rotational speed of 3120 rpm and a TRW Hartzell propeller at a rotational speed of 2360 rpm. The PSP-derived pressure coefficient distributions across the blades show a reasonable trend. Using the laser-scanning system, Liu et al. (1997b) and Torgerson et al. (1997) performed PSP measurements on rotor blades in a high-speed axial flow compressor and an Allied Signal F109 turbofan engine. PSP and TSP were applied to alternating blades, where TSP provides the temperature distributions on the blades for temperature correction of PSP. They obtained the pressure and temperature maps on the blade surfaces at different rotational speeds. The pressure distributions clearly indicate the formation of a shock on the surface as rotational speed is increased. Moshasrov et al. (1997) described PSP measurements on propellers and rotating machinery at TsAGI. Using a CCD camera system with a pulse light source, they obtained pressure distributions on propellers. PSP measurements on the helicopter rotor blades were carried out at TsAGI (Moshasrov et al. 1997) and NASA Ames.

The PSP/TSP technique provides a promising tool for measuring surface pressure distributions on a high-speed rotating blade at a high spatial resolution. Instrumentation is particularly difficult in the rotating environment and the pressure taps weaken the structure of the rotating blade. Recently, a test was performed to measure the chordwise pressure distributions on the rotor blades of a high speed axial flow compressor shown in Figure 22 (Liu et al 1996b). TSP (Ru(bpy)-Shellac) and PSP (Ru(ph_2-phen) in GE RTV

118) were applied to alternating blades. The TSP provided the temperature distributions on the blades for temperature correction of the PSP results. A scanning laser system was used for excitation and detection of luminescence. Both the TSP and PSP were excited with an Argon laser and luminescence was detected with a Hamamatsu PMT. A composite map of the temperature and pressure distributions is shown in Fig. 23. The pressure map of Figure 23 shows a strong suction surface shock wave. Comparisons to CFD over a range of rotational speeds (Figure 25) show good correlation but require care in interpretation since the error in the PSP is ~.1 psia because an in-situ calibration was not possible.

The same system was on used on an Allied Signal F109 gas turbine engine (Figure 26) giving the suction surface pressure map at 14000 rpm shown in Figure 27.

Full field rotating pressure and temperature measurements were made on blades of a 24-inch diameter scale-model fan in the NASA Lewis Research Center 9-foot by 15-foot low speed wind tunnel at rotational speeds as high as 9500 RPM (Bencic 1997). The 25% scale model used for this work was a single rotation, ultra high bypass fan. The intent of this particular test article was to evaluate a reduced tip speed fan for its acoustic signature while keeping fan performance similar to higher speed fans. The experiment was carried out by painting two blades, one with TSP and the other with PSP. The fan was operated over its designed conditions and data taken at each condition of interest. The traditional intensity based method for PSP and TSP acquisition was used requiring two images for each paint, a reference image and a data were used to determine the pressure and temperature profiles. The illumination of the PSP and TSP was performed by multiple filtered and focused xenon flashlamps. A two microseconds flash duration yielded approximately 0.5mm of blurring at the highest speeds. This amount was deemed acceptable for this test. Images were acquired using multiple flashes integrated over two hundred revolutions while the camera shutter was kept open to achieve an acceptable CCD well capacity. The painted fan blades installed in the fan test rig are shown in Figure 28. The TSP images were used to correct temperature effect on the PSP data. The temperature profiles at four speeds on the fan operating line are shown in Figure 8 and the corresponding temperature-corrected pressure images are shown in Figure 29.

Conclusion

The fundamentals and applications of the TSP and PSP techniques have been discussed in this paper. The TSP technique has been used not only to visualize surface flow features such as boundary layer transition, shocks and separation, but also to obtain quantitative surface temperature and heat transfer maps with good accuracy. Applications of the PSP technique are focused on surface pressure measurements on airfoils, generic wing-body models aircraft models and turbomachinery over a wide range of Mach numbers. The field mapping capability of the TSP and PSP techniques is able to provide information about complicated flow characteristics that cannot be easily acquired using more conventional methods. Much effort has being made to improve essential elements of the measurement system including paint formulation, illumination, imaging, and data acquisition/processing hardware and software. Many groups are working to extend and refine TSP and PSP measurements so they will become a routine procedure in aerodynamics testing.

Acknowledgment:

This work was supported by ONR, AFOSR, NASA Langley, NASA Ames, NASA Lewis and the Boeing Company.

REFERENCES

Asai, K., Kanda, H., Kunimasu, T., Liu, T. and Sullivan, J. (1997a), Detection of Boundary-Layer Transition in a Cryogenic Wind Tunnel by Using Luminescent Paint, J. of Aircraft Vol. 34, No. 1,34-42.

Asai, K., Kanda, Cunningham, C. ,Erausquinn, R.. and Sullivan, J. (1997b), Surface Pressure Measurement in a Cryogenic Wind Tunnel Using a Luminescent Coating, 17th Int. Cong. Instrumentation in Aerospace Simulation Facilities (ICIASF), Institute of Electrical and Electronics Engineers, Monterey CA., USA.

Baron, A. E., Danielson, J. D., Gouterman, M., Wan, J., Callis, J. B. and McLachlan, B. (1993), Submillisecond Response Times of Oxygen-Quenching Luminescent Coatings, Rev. Sci. Instrum. 64(12), 3394-3402.

Bell, J. H. and McLachlan, B. G. (1996), Image Registration for Luminescent Paint Sensors, EXP FLUIDS 22: (1) 78-86

Bencic, T. (1997), Rotating pressure measurements on a scale model high-by-pass ratio fan using PSP at NASA LeRC, Proceeding of the Sixth Annual Pressure Sensitive Paint Workshop, Arnold Engineering Development Center, Tullahoma, Tennessee, May 14-16.

Bennett, R. G. and McCartin, P. J. (1966), Radiationless Deactivation of the Fluorescent State of Substituted Anthracences, The Journal of Chemical Physics, Vol. 44, No. 5, 1969-1973.

Birch, D. J. S. and Imhof, R. E. (1991), Time-Domain Fluorescence Spectroscopy Using Time-Correlated Single-Photon Counting, Topics in Fluorescence Spectroscopy, Volume 1: Techniques, edited by J. R. Lakowicz, Plenum Press, New York, Chapter 1.

Borovoy, V., Bykov, A., Mosharov, V., Orlov, A., Radchenko, V. and Phonov, S. (1995), Pressure Sensitive Paint Application in Shock Wind Tunnel, Proc. 16th Int. Cong. Instrumentation in Aerospace Simulation Facilities (ICIASF), Institute of Electrical and Electronics Engineers, Wright-Patterson Air Force Base, Dayton, OH, USA, 34.1-34.4.

Bukov, A., Mosharov, V., Orlov, A., Pesetsky, V., Radchenko, V., Phonov, S., Matyash, S.,Kuzmin, M. and Sadovsky, N. (1993), Optical Surface Pressure Measurements: Accuracy and Application Field Evaluation, 73th AGARD Fluid Dynamics Panel Meeting

Campbell, B., Liu, T. and Sullivan, J. (1994), Temperature Sensitive Fluorescent Paint System, AIAA Paper 94-2483.

Carroll, B. F., Abbitt, J. D., Lukas, E. W. and Morris, M. J. (1996), Step Response of Pressure Sensitive Paints, AIAA J, Vol. 34, No. 3, 521-526.

Crites, B. C. (1993), Measurement Techniques ---- Pressure Sensitive Paint Technique, Lecture Series 1993-05, von Karman Institute for Fluid Dynamics.

Davies, A. G., Bedwell, D., Dunleavy, M. and Brownjohn, N. (1995), Pressure Sensitive Paint Measurements Using a Phosphorescence Lifetime Method, presented at Seventh International Symposium on Flow Visualization, September 11-14, Seattle, Washington.

Donovan, J. F., Morris, M. J., Pal, A., Benne, M. E. and Crites, R. C. (1993), Data Analysis Techniques for Pressure- and Temperature-Sensitive Paint, AIAA Paper 93-0176.

Dowgwillo, R. M., Morris, M. J., Donovan, J. F. and Benne, M. E. (1996), Pressure sensitive paint in transonic wind-tunnel testing of the F-, J AIRCRAFT 33: (1) 109-116 J AIRCRAFT 33: (1) 109-116.

Engler, R. H. (1995), Further Developments of Pressure Sensitive Paint (OPMS) for Non Flat Models in Steady Transonic Flow and Unsteady Conditions, Proc. 16th Int. Cong. Instrumentation in Aerospace Simulation Facilities (ICIASF), IEEE , Wright-Patterson Air Force Base, Dayton, OH, USA, 33.1-33.8.

Gouterman M, (1997)Oxygen quenching of luminescence of pressure sensitive paint for wind tunnel research, J Chem Educ 74: (6) 697-702

Hamner, M., Campbell, B., Liu, T. and Sullivan, J. (1994), A Scanning Laser System for Temperature and Pressure Sensitive Paint, AIAA Paper 94-0728.

Harris, J. and Gouterman, M. (1995), Referenced Pressure Sensitive Paint, Flow Visualization VII, Proceeding of the Seventh International Symposium on Flow Visualization, edited by J. Crowder, Seattle, Washington, p.802.

Kavandi, J., Callis, J. B., Gouterman, M. P., Khalil, G., Wright, D., Green, E., Burns, D. and McLachlan, B. (1990), Luminescent Barometry in Wind Tunnels, Rev. Sci. Instrum. 61(11), 3340-3347.

Liu, T., Campbell, B. and Sullivan, J. (1995a), Fluorescent Paint for Measurement of Heat Transfer in Shock-Turbulent Boundary Layer Interaction, Experimental Thermal and Fluid Science 10, 101-112.

Liu, T., Campbell, B. Sullivan, J. ,Lafferty, J., and Yanta, W., (1995b), Heat Transfer Measurements on a Waverider Model at Mach 10 Using Fluorescent Paint, J. Thermophys. and Heat Trans, Vol 9,No.4, 605-611.

Liu, T., Campbell, B. and Sullivan, J. (1995c), Accuracy of Temperature-Sensitive Fluorescent Paint for Heat Transfer Measurements, AIAA Paper 95-2042.

Liu, T. and Sullivan, J. (1996a), Heat Transfer and Flow Structures in an Excited Circular Impinging Jet, Int. J. Heat Mass Trans. Vol.39,No.17, 3695-3706.

Liu, T., Johnston, R., Torgerson, S., Fleeter, S. and Sullivan, J. (1996b), Rotor Blade Pressure Measurement in a High Speed Axial Compressor Using Pressure and Temperature Sensitive Paint, AIAA Paper 97-0162.

Liu, T., Campbell, T. Burns, S. ,and Sullivan, J. (1997), Temperature and Pressure Sensitive Luminescent Paints in Aerodynamics, App Mech. Rev. Vol 50, No 4, 227-246.

Liu, T., Guille, M., and Sullivan, J. (1999), Accuracy of Pressure Sensitive Paint, AIAA Paper 99-3785.

McLachlan, B. G., Kavandi, J. L., Callis, J. B., Gouterman, M., Green, E. and Khalil, G. (1993a), Surface Pressure Field Mapping Using Luminescent Coatings, Experiments in Fluids 14, 33-41.

McLachlan, B. G., Bell, J. H., Gallery, J., Gouterman, M. and Callis, J. (1993b), Boundary Layer Transition Detection by Luminescence Imaging, AIAA Paper 93-0177.

McLachlan, B. G. and Bell, J. H. (1995a), Pressure-Sensitive Paint in Aerodynamic Testing, Experimental Thermal and Fluid Science, 10, 470-485.

McLachlan, B. G., Bell, J. H., Park, H., Kennelly, R. A., Schreiner, J. A., Smith, S. C., Strong, J. M., Gallery, J. and Gouterman, M. (1995b), Pressure-Sensitive Paint Measurements on Supersonic High-Sweep Oblique Wing Model, Journal of Aircraft, Vol. 32, No. 2, March-April, 217-227.

Morris, M. J., Benne, M. E., Crites, R. C. and Donovan, J. F. (1993a), Aerodynamics Measurements Based on Photoluminescence, AIAA Paper 93-0175.

Morris, M. J., Donovan, J. F., Kegelman, J. T., Schwab, S. D., Levy, R. L. and Crites, R. C. (1993b), Aerodynamic Applications of Pressure Sensitive Paint, AIAA Journal, Vol. 31, No. 3, March, 419-425.

Morris, M. J. (1995), Use of Pressure-Sensitive Paints in Low-Speed Flows, Proc. 16th Int. Cong. Instrumentation in Aerospace Simulation Facilities (ICIASF), Institute of Electrical and Electronics Engineers, Wright-Patterson Air Force Base, Dayton, OH, USA, 31.1-31.10.

Mosharov, V. E., Radchenko, V. N. and Fonov, S. D. (1997), Luminescent Pressure Sensors in Aerodynamic Experiments, Central Aerohydrodynamic Institute (TsAGI), CWA International Corporation, Moscow.

Oglesby, D. M., Leighty, B. D. and Upchurch, B. T. (1995), Pressure Sensitive Paint With an Internal Reference Luminiphore, Proceedings of the 41st International Instrumentation Symposium, Instrument Society of America, Denver, CO, 381-395.

Oglesby, D. M., Upchurch, B. T., Leighty, B. D. and Simmons, K. A. (1996), Pressure Sensitive Paint With Internal Temperature Sensing Luminiphore, Proceedings of the 42nd International Instrumentation Symposium, Instrument Society of America, San Diego, CA.

Popernack, T, ,Owens, L., Hamner, M. ,Morris, M.,(1997) Application of Temperature Sensitive Paint for Detection of Boundary Layer Transition, 17th Int. Cong. Instrumentation in Aerospace Simulation Facilities (ICIASF), Institute of Electrical and Electronics Engineers, Monterey CA., USA.

Papkovsky, D. B. (1995), New Oxygen Sensors and Their Application to Biosensing, Sensors and Actuators B, 29, 213-218.

Sajben, M. (1993), Uncertainty Estimates for Pressure Sensitive Paint Measurements, AIAA J., Vol. 31, No. 11, 2105-2110.

Schanze KS, Carroll BF, Korotkevitch S, et al.,(1997) Temperature dependence of pressure sensitive paints, AIAA J 35: (2) 306-310

Scroggin, A. M., Slamovich, E. B., Crafton, J. W., Lachendro, N., Sullivan, J. P. (1999) "Porous Polymer / Ceramic Composites for Luminescence-Based Temperature and Pressure Measurement", Materials Research Society Symposium Proceedings,

Shimbo, Y. , Mehta, R. Cantwell, B. (1997), Vortical Flowfield Investigation Using Pressure Sensitive Painnt Technique at Low Speed, AIAA Paper 97-0388.

Sellers, M. E. and Brill, J. A. (1994), Demonstration Test of Pressure Sensitive Paint in the AEDC 16-ft Transonic Wind Tunnel Using the TST Model, AIAA Paper 94-2481.

Szmacinski, H. and Lakowicz, J. R. (1995), Fluorescence Lifetime-Based Sensing and Imaging, Sensors and Actuators B, 29, 16-24.

Torgerson, S. D., Liu, T. and Sullivan, J. P. (1996), Use of Pressure Sensitive Paints in Low Speed Flows, AIAA Paper 96-2184.

Torgerson, S. D. (1997), Laser Scanning System for use with pressure and temperature sensitive paint. MS Thesis, Sch of Aero and Astro, Purdue Univ, W. Lafayette IN.

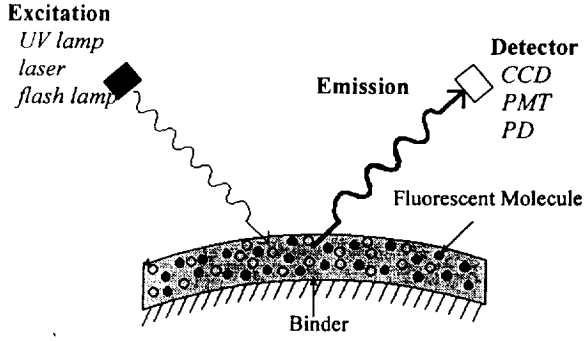

Figure 1: Schematic of TSP/PSP Layer

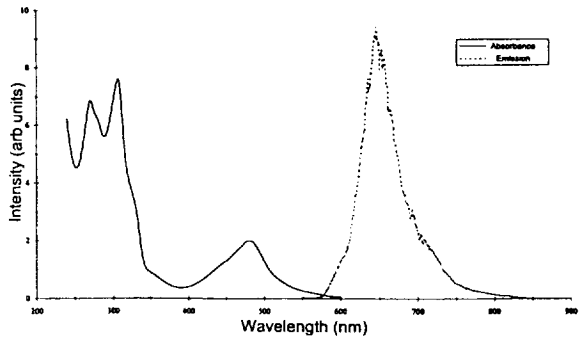

Figure 2: Excitation and Emission spectra of a Ruthenium based molecule

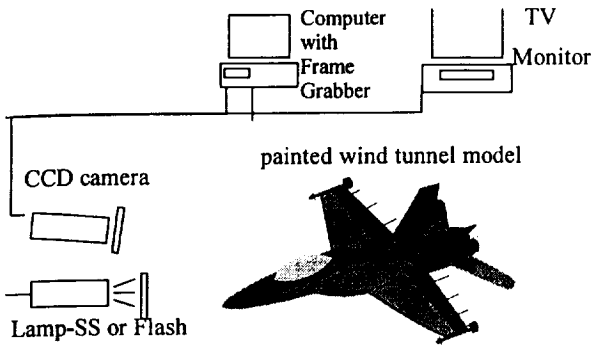

Figure 3: Schematic of CCD camera system

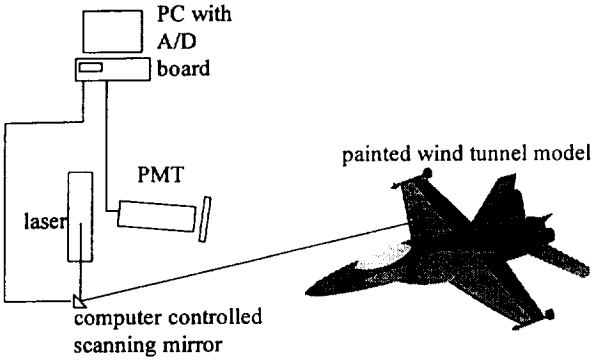

Figure 4: Schematic of laser scanning system

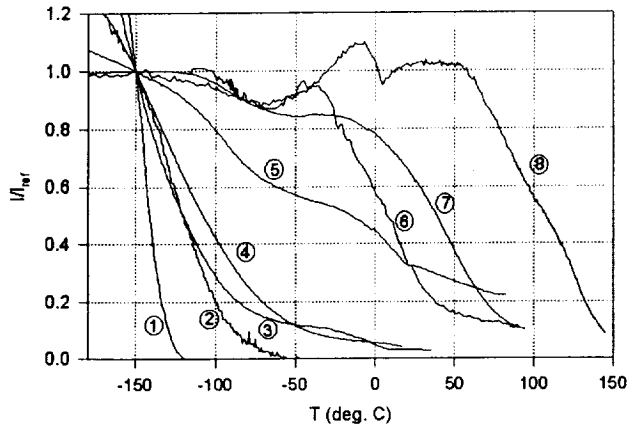

Figure 5.Temperature dependence of luminescence intensity for several TSP formulations: (1) Ru(trpy) in Ethanol/ Methanol, (2) Ru(trpy)(phtrpy) in GP-197, (3) Ru(VH127) in GP-197, (4) Ru(trpy) in Du Pont Chroma Clear, (5) Ru(trpy)/Zeolite in GP-197, (6) EuTTA in dope, (7) Ru(bpy) in Du Pont Chroma Clear, (8) Perylenedicarboximide in Sucrose Octaacetate. (T_{ref} = -150 °C).

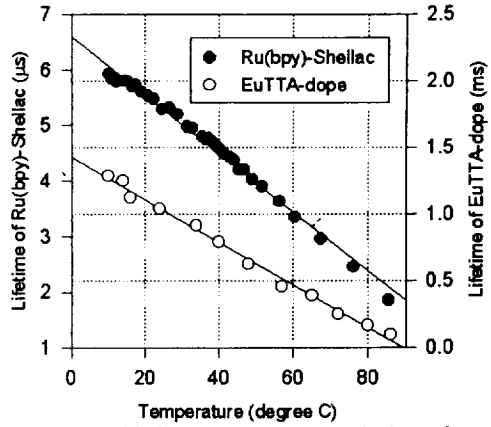

Figure 6 Lifetime-temperature relations for Ru(bpy)-Shellac and EuTTA-dope paints.

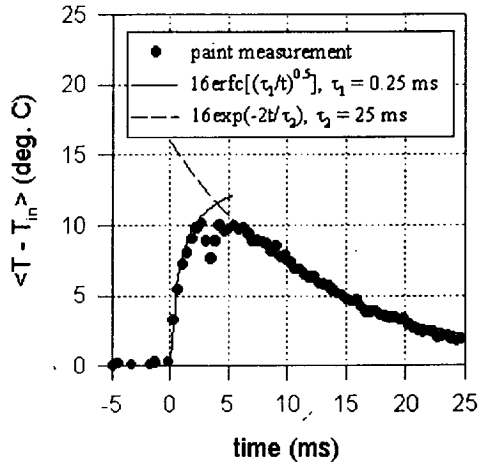

Figure 7 Temperature response of Ru(bpy)-Shellac paint to pulsed laser heating on steel foil.

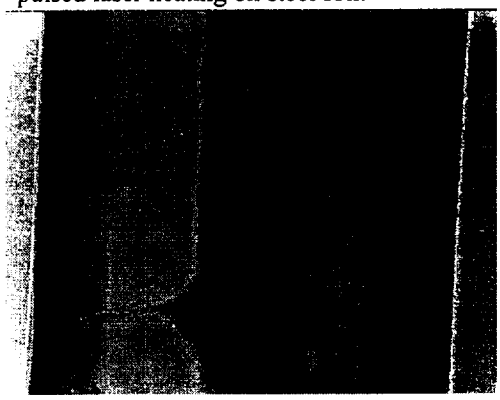

Figure 8. Transition at low speed on a NACA 65-021 Airfoil

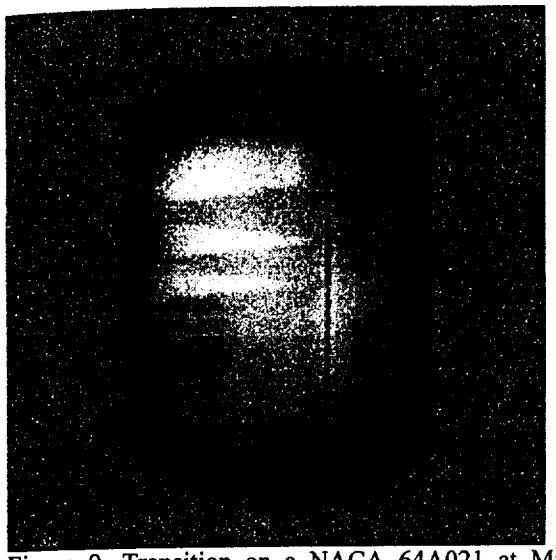

Figure 9. Transition on a NACA 64A021 at M=.82 and T=120 K in NAL cryogenic wind tunnel.

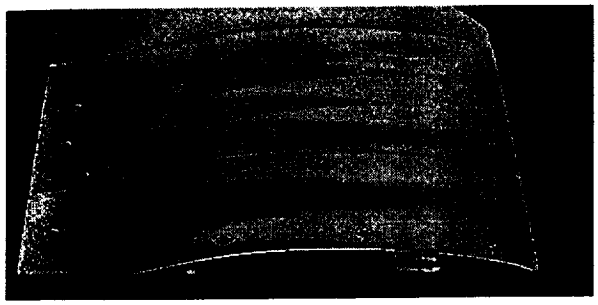

Figure 10. Transition on a HSNLF in the NASA .3 meter cryogenic wind tunnel.

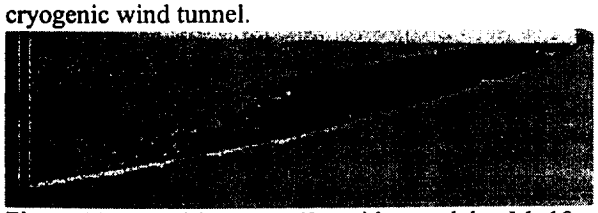

Figure 11. Transition on a Waverider model at M=10.

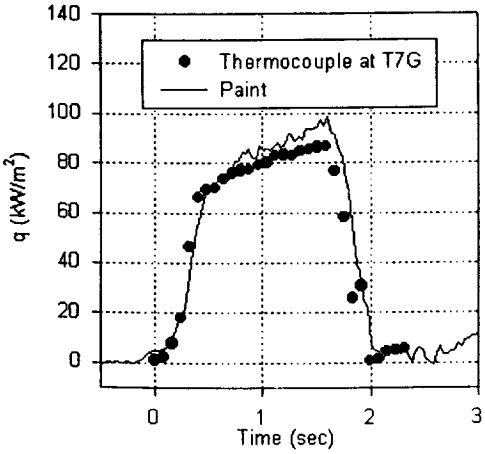

Figure 12 Heat transfer history on a Mach 10 waverider model at location T7G.

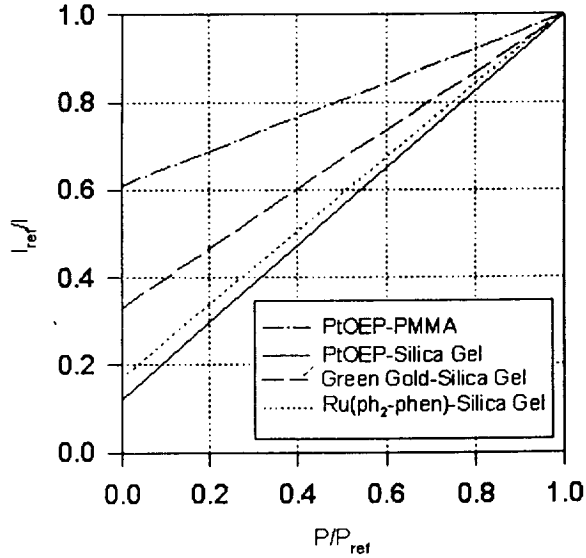

Figure 13 Stern-Volmer plots for several PSPs at ambient temperature (22 °C), where P_{ref} is the ambient pressure and I_{ref} is the luminescence intensity at ambient conditions.

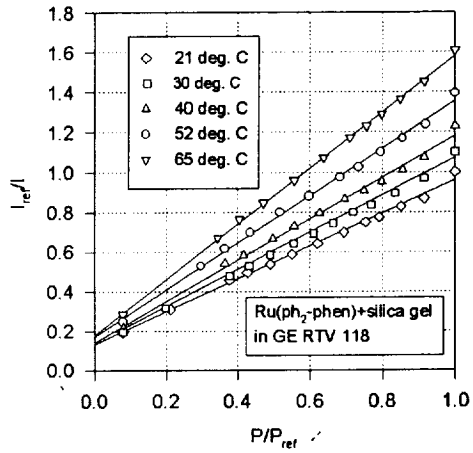

Figure 14. Calibration of Ruthenium based PSP.

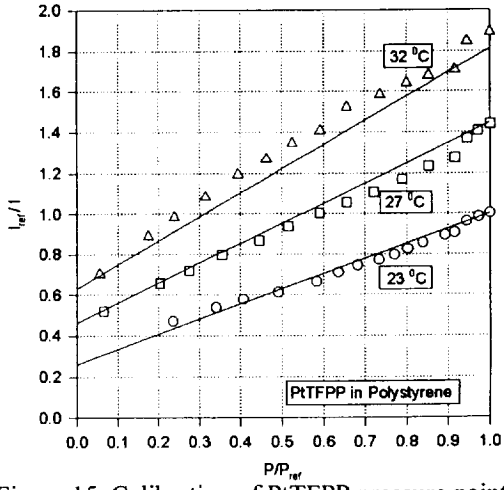

Figure 15. Calibration of PtTFPP pressure paint.

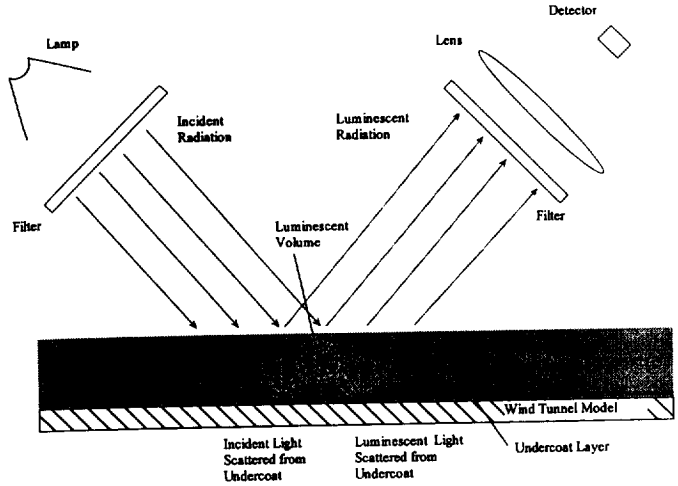

Figure 16. PSP system model.

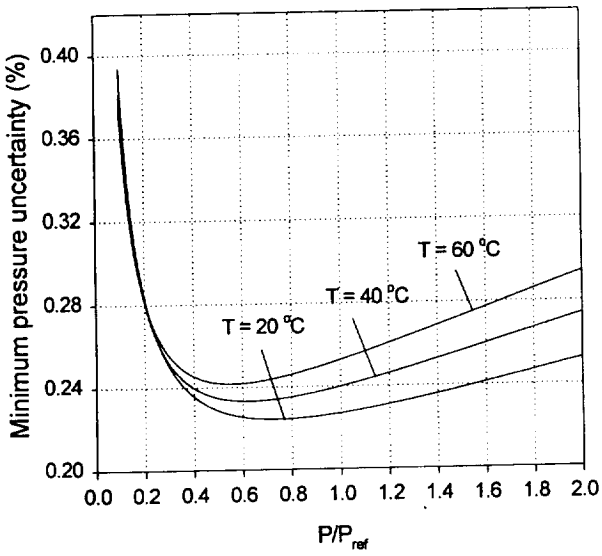

Figure 17. Shot noise limited error in PSP measurement.

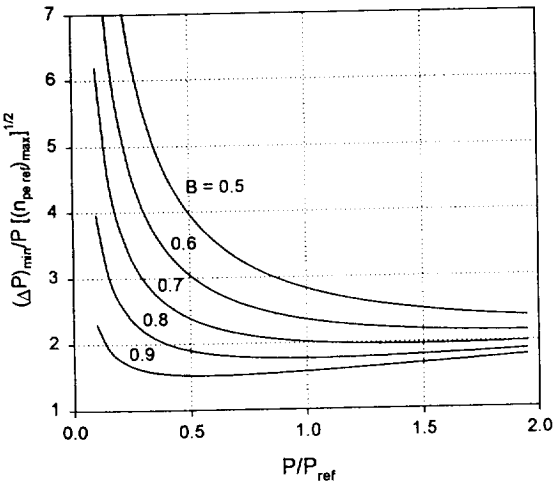

Figure 18. Effect of Stern-Volmer constant on shot noise limited error.

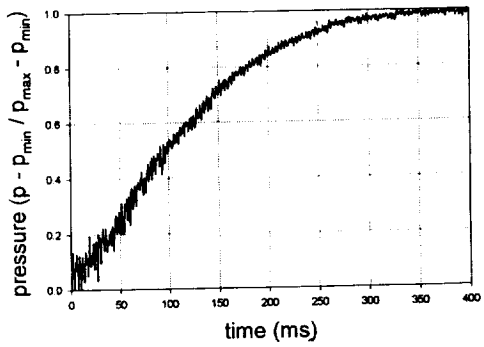

a. The response time is172 ms.for Ru(dpp) in RTV.

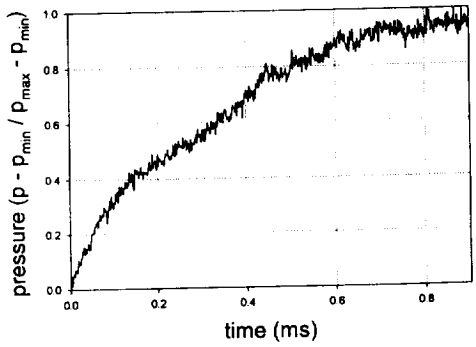

b. The response time is 349μs (PtTFPP) in porous polymer/ceramic composites.

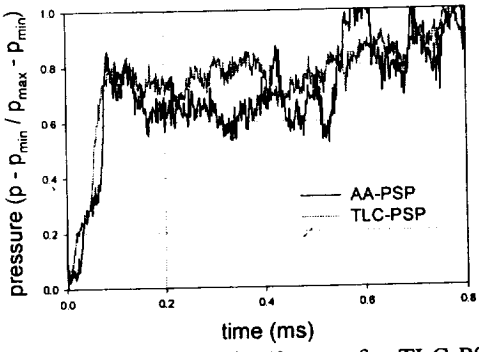

c. The response time is 70 μsec for TLC-PSP and 80 μsec for AA-PSP.

Figure 19. Time response of various paints from shock tube measurements.

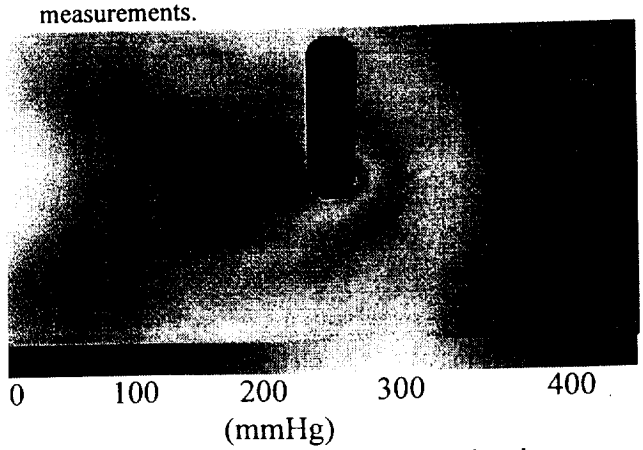

Figure 20. Pressure map for cylinder/boundary layer interaction at M=2.5.

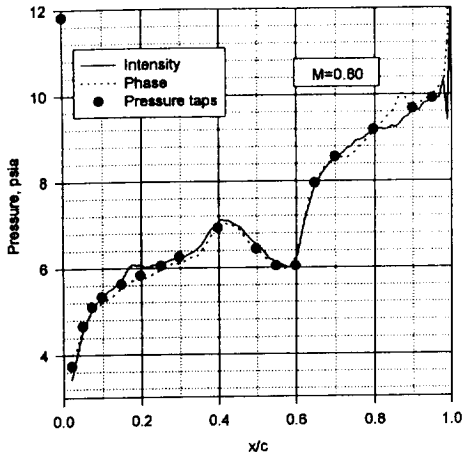

Figure 21. Pressure distribution on a transonic airfoil using both intensity and lifetime based methods.

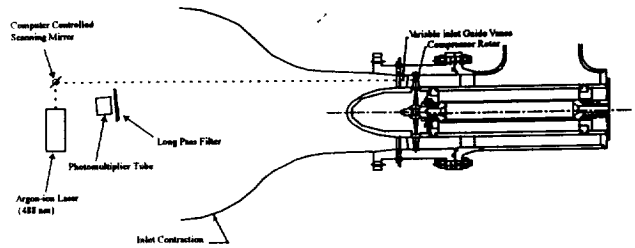

Figure 22. Transonic compressor rig with laser scanning system

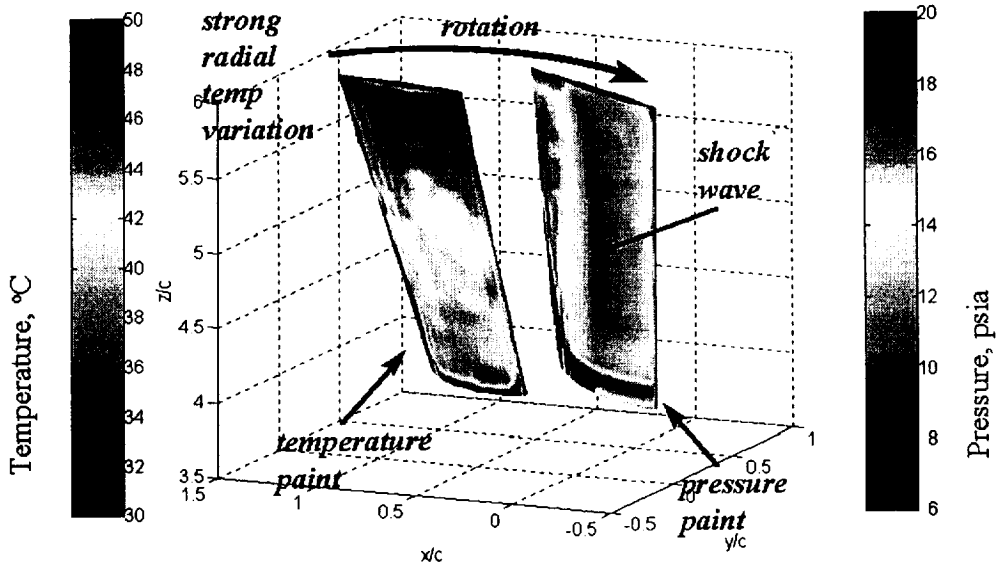

Figure 23. Temperature and pressure distribution on transonic compressor blades.

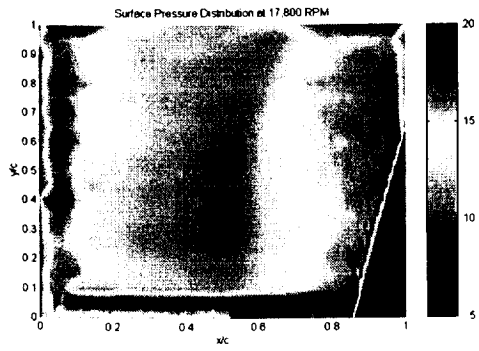

Figure24. Compressor blade suction surface pressure map at 17,800 rpm (scale in psia).

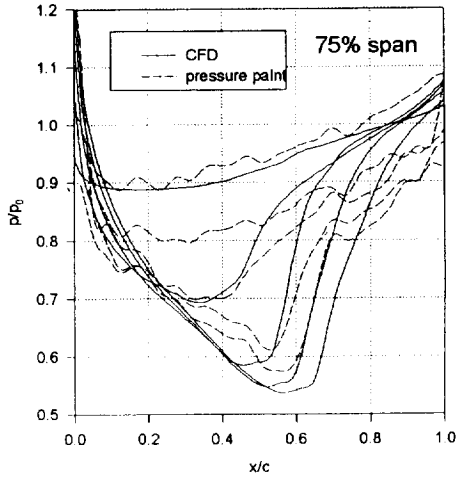

Figure 25. Comparison of PSP data and CFD results.

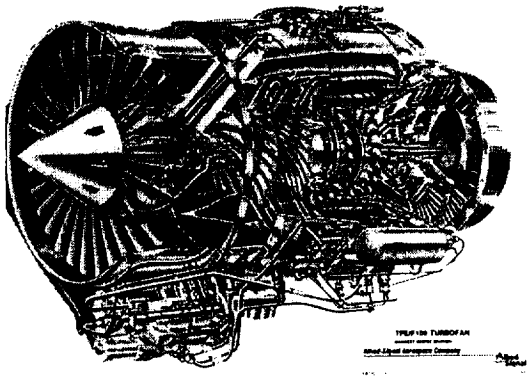

Figure 26. Allied F109 turbofan engine.

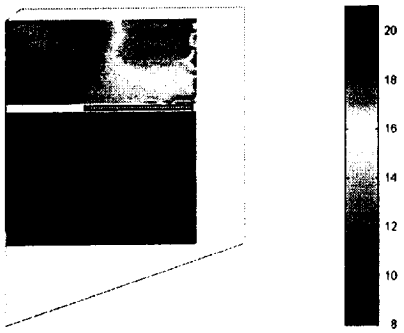

Figure 27. Fan blade pressure distribution at 14,000rpm (scale in psia).

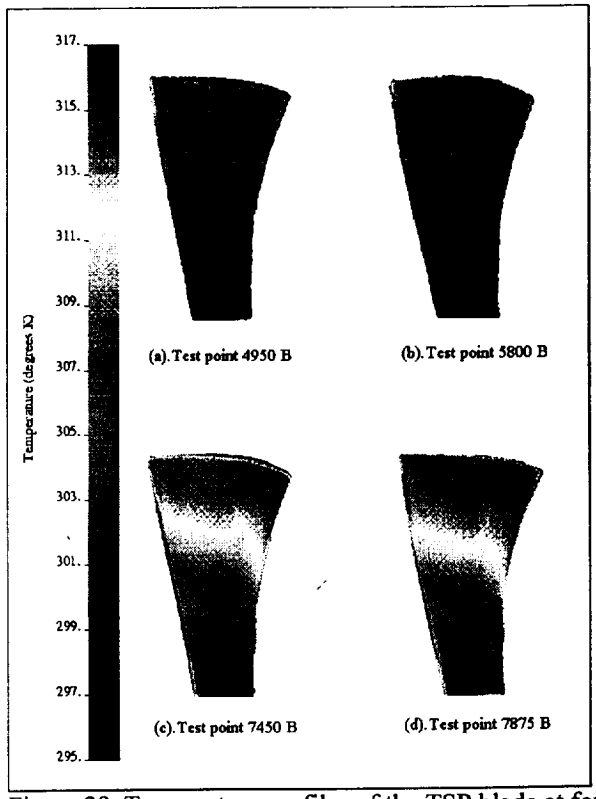

Figure 28. Temperature profiles of the TSP blade at four rig speeds.

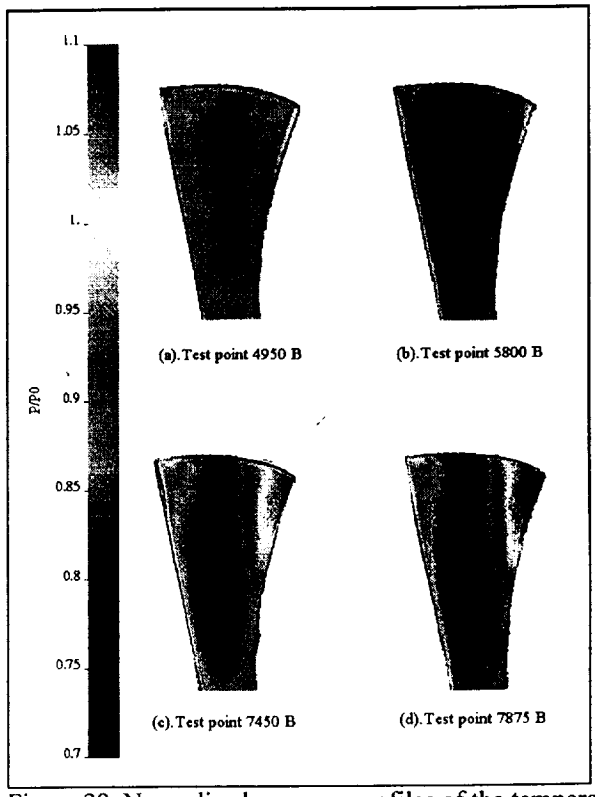

Figure 29. Normalized pressure profiles of the temperature corrected PSP blade at four rig speeds.

PURDUE UNIVERSITY

SCHOOL OF AERONAUTICS
AND ASTRONAUTICS

Chee Tung
NASA Ames Research Center
MS T12B
MOFFETT FIELD, CA 94035
United States of America

October 2, 1999

Dear Chee,

Enclosed is the final report on NCC2-5208 (Purdue 520 1282-0757) PRESSURE AND TEMPERATURE SENSITIVE PAINT MEASUREMENTS ON ROTORS

We still plan on coming to Ames for a rotor test after the first of the year as we discussed yesterday.

Sincerely,

John Sullivan
Professor
Purdue University

CC. Peter Dunn

1282 GRISSOM HALL • WEST LAFAYETTE, IN 47907-1282
(765) 494-5117 • FAX (765) 494-0307